Environ Sci Pollut Res
DOI 10.1007/s11356-015-4932-6

Coastal hydrogeological system of Mar Piccolo (Taranto, Italy)

L. E. Zuffianò[1] · A. Basso[1] · D. Casarano[1] · V. Dragone[1] · P. P. Limoni[1] · A. Romanazzi[1] · F. Santaloia[1] · M. Polemio[1]

Received: 13 March 2015 / Accepted: 19 June 2015

Abstract The Mar Piccolo basin is an internal sea basin located along the Ionian coast (Southern Italy), and it is surrounded primarily by fractured carbonate karstic environment. Because of the karstic features, the main continental water inflow is from groundwater discharge. The Mar Piccolo basin represents a peculiar and sensitive environment and a social emergency because of sea water and sediment pollution. This pollution appears to be caused by the overlapping effects of dangerous anthropogenic activities, including heavy industries and commercial and navy dockyards. The paper aims to define the contribution of subaerial and submarine coastal springs to the hydrological dynamic equilibrium of this internal sea basin. A general approach was defined, including a hydrogeological basin border assessment to detect inflowing springs, detailed geological and hydrogeological conceptualisation, in situ submarine and subaerial spring measurements, and flow numerical modelling. Multiple sources of data were obtained to define a relevant geodatabase, and it contained information on approximately 2000 wells, located in the study area (1600 km^2). The conceptualisation of the hydrogeological basin, which is 978 km^2 wide, was supported by a 3D geological model that interpolated 716 stratigraphic logs. The variability in hydraulic conductivity was determined using hundreds of pumping tests. Five surveys were performed to acquire hydro-geochemical data and spring flow-yield measurements; the isotope groundwater age was assessed and used for model validation. The mean annual volume exchanged by the hydrogeological basin was assessed equal to 106.93 10^6 m^3. The numerical modelling permitted an assessment of the mean monthly yield of each spring outflow (surveyed or not), travel time, and main path flow.

Keywords Coastal water quality · Karstic coastal aquifer · Spring yield · Groundwater modelling · Mediterranean Sea · Italy · Apulia · Subaerial and submarine springs

Responsible editor: Marcus Schulz

✉ M. Polemio
m.polemio@ba.irpi.cnr.it

[1] Istituto di Ricerca per la Protezione Idrogeologica – CNR, Bari, Italy

Introduction

The Mar Piccolo ('little sea', approximately 20.7 km^2) basin is a small marine basin that lies to the north of Taranto (southern Italy; Fig. 1) and is currently connected to the open sea (Ionian Sea) through two channels. Taranto is the main industrial town of the Apulian Region, and it has hosted a primary navy dockyard since 1865 and commercial dockyards and heavy industries for decades. These key activities have contributed to worsening the quality of the air, water and sediments of this Ionian coastal sector. For instance, industrial waste was deposited in abandoned quarries for decades or allowed to temporarily accumulate on the ground surface because of a lack of awareness of pollution risks. In addition, agricultural fertilisers and pesticides and civil sewage disposal were potential sources of groundwater pollutants. Therefore, sea water and sediments have been contaminated (Cardellicchio et al. 2007), and the polluted environment continues to pose a threat to the health of the local inhabitants of the Taranto area, and it causes economic losses, such as the reduced production of seafood, and social damage, such as a lack of employment because of issues surrounding polluting heavy industries. Because of such economic and environmental consequences, the scientific community has begun to analyse all of the complex processes occurring in the Mar Piccolo ecosystem. Several subaerial and submarine springs are located in the Mar Piccolo

Published online: 24 July 2015

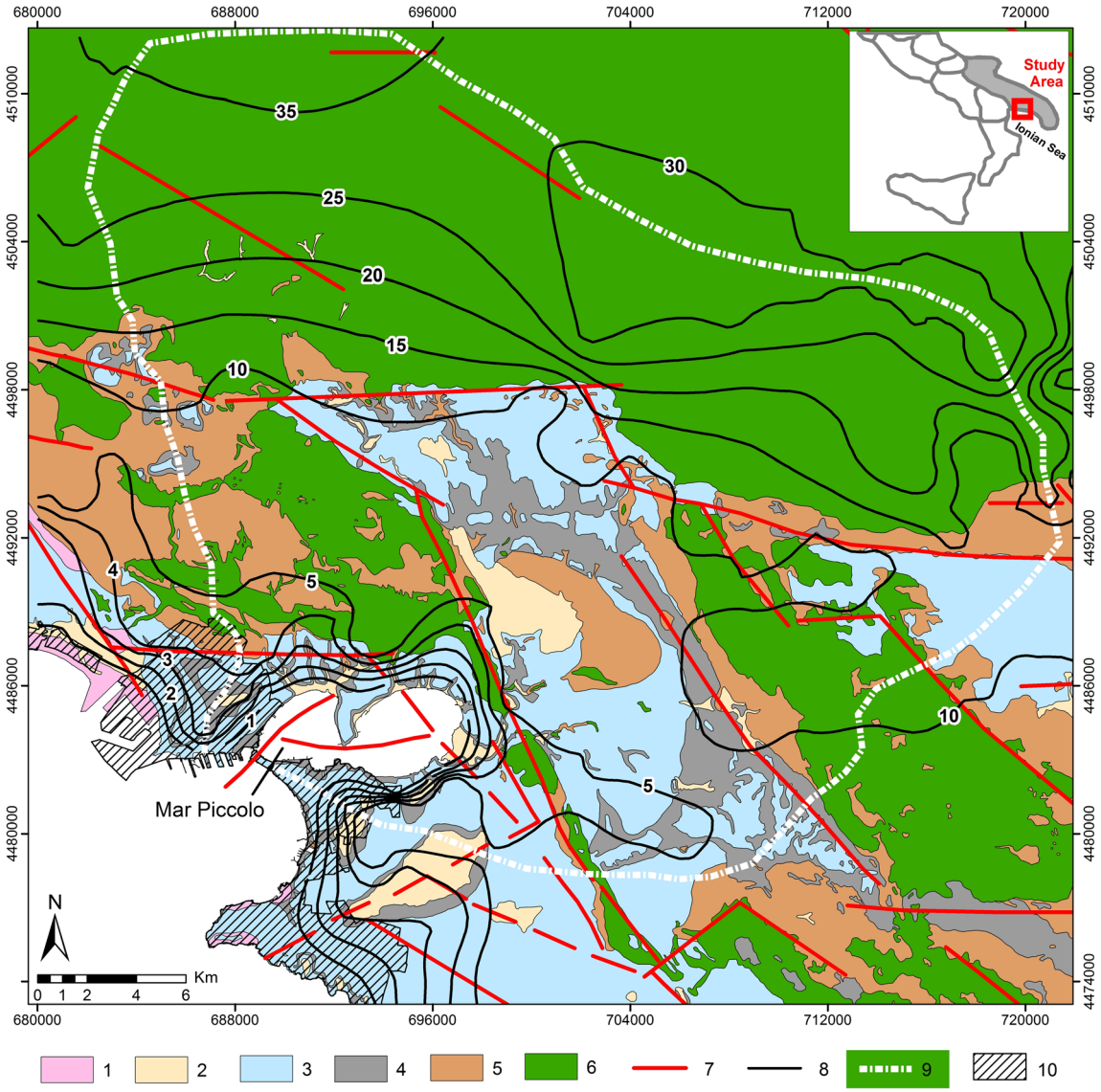

Fig. 1 Geological and hydrogeological map of the study area (modified after Ciaranfi et al. 1988; Cotecchia et al. 1989; CNR 1987). *1*) Holocene coastal deposits, 2) Holocene alluvial deposits, *3*) Middle and Upper Pleistocene calcarenite and sand (terraced marine deposits), *4*) Lower Pleistocene clay (Subappennine clays, *5*) Middle Pliocene-Lower Pleistocene calcarenite (Gravina calcarenite), *6*) Cretaceous limestone (Altamura limestone), *7*) fault, *8*) piezometric head, *9*) groundwater divide, and *10*) urbanised and industrialised area of Taranto. Upper right map: southern area, Apulian region (grey filling), and study area

basin, and they contribute to the peculiar hydrogeological environment, which will be discussed subsequently.

Fresh groundwater discharge into seas and lagoons is estimated to account for approximately 6 % of the river discharge worldwide (Polemio and Limoni 2006). This low percentage of groundwater discharge can be misleading if areas with high permeability with outcrops of highly fractured and karstic carbonate rocks are considered.

The percentage of coastal groundwater discharge is very large in these environments. In these cases, the coastal groundwater discharge is remarkable because of its effects on the hydrological and ecological equilibrium of humid environments located near the coast (UNESCO 2004; Sanford et al. 2007). These effects include variations in the quantity and quality of groundwater resources; seawater intrusions that withdraw or move inland with increases or decreases in coastal groundwater discharge respectively; seawater intrusion interface movements that affect the salinity of the coastal springs; variations in groundwater discharge and/or salinity that influence the chemical characteristics of coastal-surface waters and produce ecologically complex effects that are often dramatic in valuable humid habitats; groundwater transport of contaminants and nutrients from inland ground surface to surface coastal waters.

In primarily karstic environments, infiltration is greater than runoff; in the karstic coastal Apulian aquifers, the

groundwater discharge to the sea is more than twofold greater than the surface discharge, notwithstanding the high discharges by wells (Polemio and Limoni 2006; Polemio et al. 2008). In such environments, including the Mar Piccolo area, the quantity and quality of groundwater outflow caused by of coastal submarine and subaerial discharge play key roles in the ecological equilibrium of these coastal environmental systems (Polemio and Limoni 2001) and are particularly important for biodiversity and environmental protection.

The main goal of this paper was to define the groundwater contribution to the hydrological dynamic equilibrium of the Mar Piccolo basin to be used by other research groups of RITMARE Project (details in the acknowledgements), as input for hydrological numerical modelling of this protected sea basin. Thus, a methodological approach was defined and applied to the study case, which is dominated by the effects of a wide and deep limestone coastal aquifer composed of the Murgia carbonate hydrogeological structure (Cotecchia et al. 2005; Polemio et al. 2009) and outcrops of shallow secondary porous aquifers (Polemio 1998). The main aquifer constitutes primary local water source and feeds numerous coastal springs, many of which are submarine.

Methodological approach

The proposed approach can be applied to other study areas in which coastal groundwater outflow is the primary input, and it is relevant for determining the hydrological and ecological equilibria of coastal-surface water systems (COST 2005; Polemio and Limoni 2006). The approach can be represented as a sequence of steps.

Using all of the available geological, hydrogeological and hydro-geochemical sources of data (Castany 1982), which were primarily scientific papers and maps, technical reports, monitoring databases and institutional studies (performed by the Geological Survey and local and national authorities), a geodatabase should be constructed. However, these data must be verified as sufficient to define the qualitative and quantitative contributions of groundwater discharge to the selected coastal water environment.

If such data are insufficient, which is the case worldwide, particularly in areas dominated by high-permeability coastal aquifers, two types of activities should be designed and performed: survey activities and 3D numerical modelling (an exhaustive reference list cannot be included here; however, recommended references include Anderson and Woessner 1992; ASCE 1996; Fetter 2001; Todd and Mays 2005; Appelo and Postma 2005; Civita 2005).

Survey activities should be finalised to fill in any gaps in terms of monitoring data on coastal spring outflow, and the surveys should concentrate on the quality and quantity of discharge into the sea. Thus, multiple tools, equipment and methods should be used, although a detailed general description is not within the scope of the paper. The survey activities should be designed to obtain a reliable assessment of the quality and quantity of groundwater discharge from the primary springs. Spring outflow measurements, spring groundwater age assessments and piezometric data are required to calibrate and validate numerical groundwater models.

A divide assessment of the hydrogeological basin and conceptualisation of the hydrogeological conditions should be performed. Subsequently, an assessment of the hydrological budget and study of the spatial variability of hydrogeological parameters (primarily hydrogeological conductivity) should be performed (ASCE 1996; Civita 2005).

3D numerical modelling activities should then be conducted to integrate all of the data and provide a detailed study of each hydrological and ecological phenomenon that affects the selected coastal water environment.

Accurate flow and transport numerical models for large or regional aquifers are based on the equivalent porous medium hypothesis (Langevin 2003; Romanazzi and Polemio 2013); such models can also be used for karstic aquifers (Abbo et al. 2003; Scanlon et al. 2003). The open-source program MODFLOW (McDonald and Harbaugh 1988), which is a three-dimensional finite-difference groundwater flow model, may be considered a worldwide standard model. In addition, complementary programs such as PEST (Doherty 2002), which is used for model calibration, and MODPATH (Pollock 1989), which is used to assess flow path and flow time, could also be implemented.

This approach was fully applied to the study case.

Geological and hydrogeological features of the study area

The Mar Piccolo basin is divided by a north–south oriented promontory in two almost elliptical bays. The western bay is connected to the open sea by two channels, which separate the land upon which the historical centre of Taranto City was constructed (Fig. 1). The average seawater salinity is approximately 3.5 %, which is 0.2 % less than that of the close outer sea because of the inflow of fresh spring water (Annichiarico et al. 2009). At the bottom of the Mar Piccolo basin are submarine springs, which are locally referred to as *citri*. Common characteristics of *citri* are outflow that occur across a roughly circular hole on the sea bottom (main *citri* shows diameter of several m up to 20 m and sea bottom at maximum depth of 33 m), deep and steep inverted cone surface that can be observed below the hole, and groundwater velocity that is so high that the outflow effect on the seawater surface can be observed with the naked eye (Panetta and Dell'Angelo 1975; Cotecchia et al. 1989). Small *citri* and an almost diffuse seepage were also observed (Cerruti 1938). In terms of spring

outflow yield, discontinuous data were available for certain subaerial coastal springs (Servizio 1953), and only a limited number of measurements were available for one *citro* (Cotecchia et al. 1989). The limited availability of previous data requires survey activities and 3D numerical modelling to be performed.

The study area, about 1600 km^2 wide, is located between the Ionian Sea and southwestern sector of the Apulian Foreland, which is the foreland of the southern Apennines. The main geological units outcropping in this area are (from the bottom to the top) (Fig. 1): Cretaceous limestone (Altamura limestone), Upper Pliocene-Lower Pleistocene calcarenites, (Gravina calcarenite), Lower Pleistocene clays (Subappenine clays), Middle-Upper Pleistocene calcarenites and sands (terraced marine deposits), Holocene alluvial deposits and coastal deposits (Ciaranfi et al. 1988).

The area is dislocated by several normal faults, which create a *horst* and *graben* setting, with tectonic structures along an almost NW-SE orientation. Plio-Quaternary deposits outcrop on the structural low sectors of the area, and Cretaceous limestone is found on the highest structural sectors. The recent sedimentary outcrops often conceal the faulted Mesozoic successions; therefore, the structural features of the tectonic structures involving these buried sequences are not easily recognisable (CNR 1987; Cotecchia et al. 1989).

The morphology of the area is defined by a series of flat surfaces gently sloping towards the sea divided by high sloping scarps and is mapped by a digital elevation model that was created for the study area, as shown in Fig. 2.

A 75-m grid-cell digital elevation model (DEM) was integrated with bathymetric data to obtain a representation of the continuous surface, merging ground surface and sea bottom surface (Fig. 2). These surfaces provided useful georeferencing log data, refined the conceptualisation, and supported numerical modelling in the submerged areas.

To provide a detailed definition of the geological and hydrogeological setting of the study area, well and boring data from approximately 2000 boreholes were collected, validated and uploaded. The stratigraphic logs were from different boring techniques, such as rotary drilling with core recovery, and percussion techniques, such as cutting recovery. Therefore, the stratigraphic data were affected by uncertainties, and these rough data were validated in detail. In particular, historical regional information on the geological setting of the area and field survey data were used to support the validation. The final geodatabase included 716 stratigraphic logs from several m to 400 m in depth, maps of the geological outcropping boundaries and geomorphological and tectonic features and detailed data that was in situ verified. The geological data were referenced with stratigraphic units that have homogeneous characteristics using lithological and chronostratigraphic criteria. The spatial trend of these units at depth was interpolated with the mapped geological outcropping boundaries and geomorphological and tectonic features to obtain a three-dimensional geological model of the entire study area (Fig. 3).

Four hydrogeological complexes were recognised (Cotecchia et al. 1989, 2005; Polemio and Romanazzi 1999): limestone, calcarenite, clay, and sand-conglomerate-calcarenite complexes (Fig. 4).

Pumping tests of 954 wells, 886 of which are connected to the limestone complex aquifer, realised generally in steady-state flow conditions, were validated and uploaded to the geodatabase to define and assess the complex characteristics and spatial variability of the hydraulic conductivity; the traditional Dupuit method was basically used to assess the hydraulic conductivity (Castany 1982). Statistics values of limestone hydraulic conductivity assessed by pumping tests are (m/s): minimum 2.1 10^{-6}, median 5.6 10^{-4}, mean 2.1 10^{-3}, peak 1.2 10^{-1}, standard deviation 0.0082.

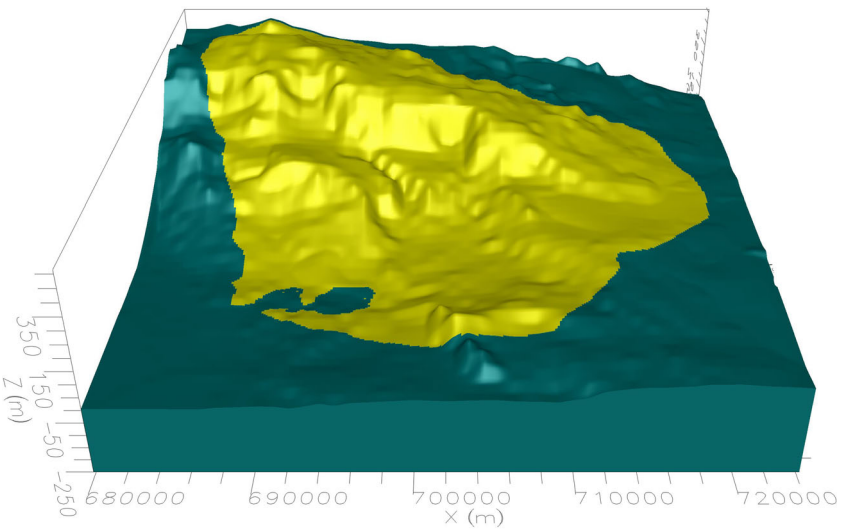

Fig. 2 Digital elevation model of the study area (vertical/horizontal scale ratio=20) and hydrogeological basin of Mar Piccolo (yellow area)

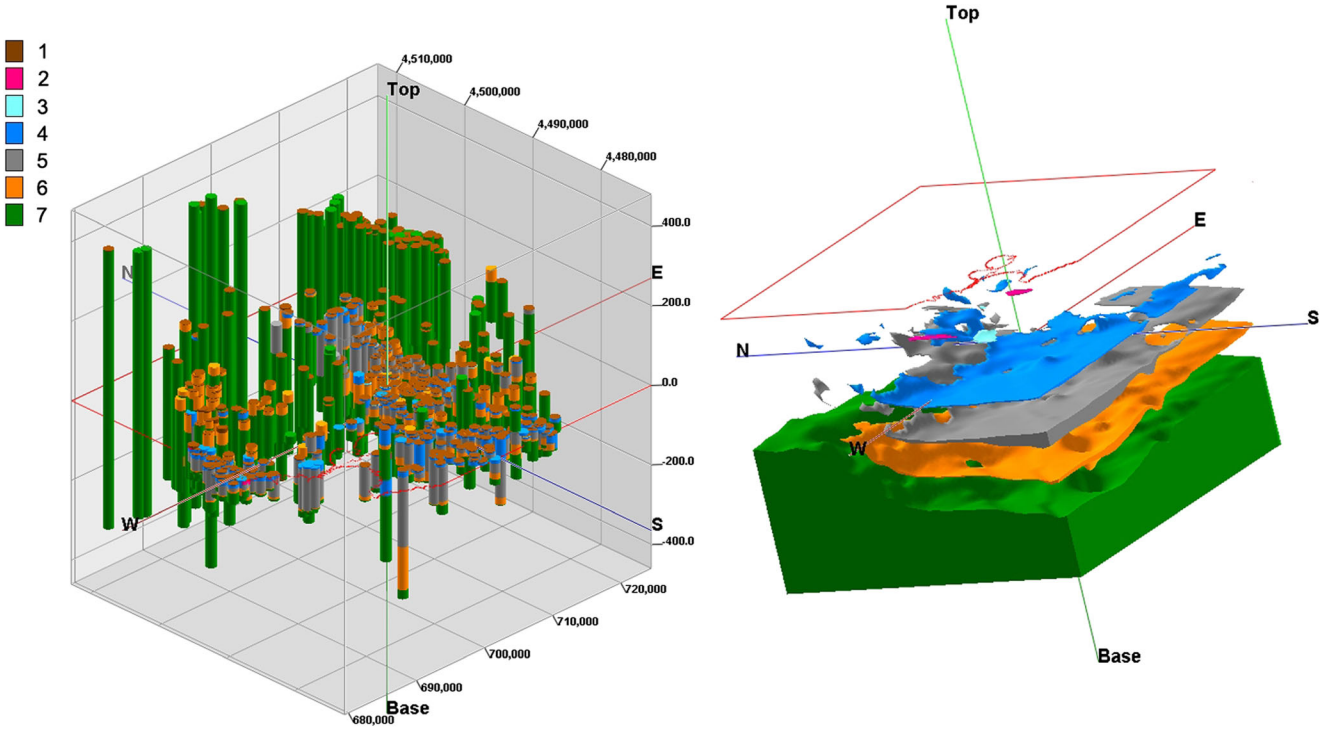

Fig. 3 3D view of the study area: geological data and interpretation. **a** 3D view of stratigraphic logs: *1*) soil, *2*) recent Holocene coastal deposits, *3*) Holocene alluvial deposits, *4*) Middle and Upper Pleistocene calcarenite and sand, *5*) Lower Pleistocene clay; *6*) Middle Pliocene-Lower Pleistocene calcarenite; and *7*) Mesozoic limestone. **b** 3D expanded representation of the main geological units

The limestone complex consists of carbonate rocks characterised by high permeability caused by fracturing and karstic processes. Resulted in the most permeable complex of the studied area, it outcrops inland and is locally overlaid by the calcarenite complex or directly by the clay complex moving towards the coastline (Fig. 5). The bottom of the limestone complex not intercepted by the studied wells is located at very high depths, some thousands of metres (Ciaranfi et al. 1988). The groundwater flow is almost negligible at some hundreds of metres depth (Cotecchia et al.

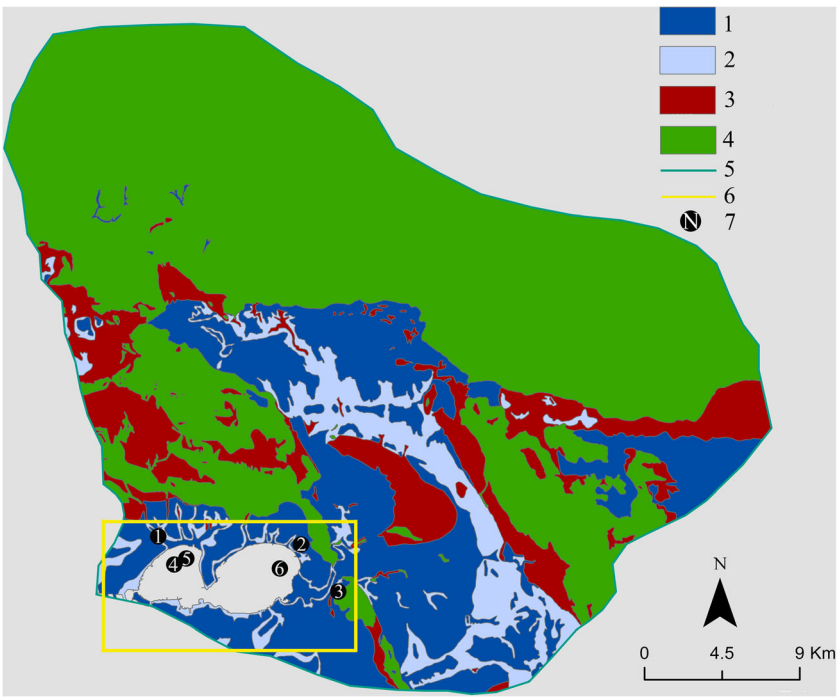

Fig. 4 Main springs and hydrogeological complexes: *1*) sand, conglomerate, and calcarenite complex; *2*) clay complex; *3*) calcarenite complex; *4*) limestone complex; *5*) hydrogeological boundary of the Mar Piccolo hydrogeological basin; *6*) detailed view of Fig. 8; *7*) subaerial springs (*1*) Galeso, (*2*) Battentieri, and (*3*) Riso and submarine springs (*4*) Citro Galeso, (*5*) Citrello, and (*6*) Citro Le Copre

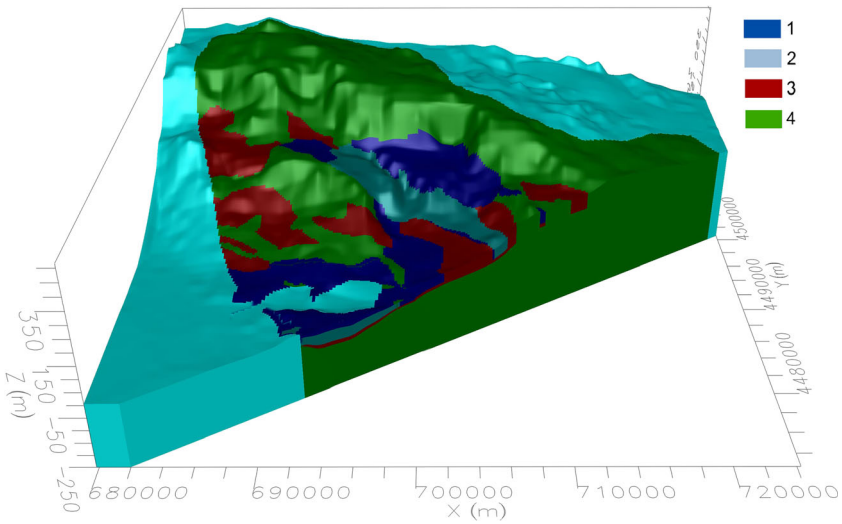

Fig. 5 Cross section and 3D view of the hydrogeological conceptualisation. Hydrogeological complexes: *1*) sand-conglomerate-calcarenite complex; *2*) clay complex; *3*) calcarenite complex; and 4) limestone complex

2005). This complex corresponds to the deep limestone aquifer that partially constitutes the Mar Piccolo hydrogeological basin (Fig. 1).

The calcarenite complex outcrops in the central sector of the study area and lies over the previous complex, and it is locally covered by the clay complex. The calcarenite complex has an average thickness of 20 m (35 m maximum thickness) and exhibits low to medium-high permeability, with the highest permeability values recorded in the fractured calcarenite. This complex behaves as a permeable top of the deep limestone aquifer.

Grey-blue clays and locally sandy or silty clays that are distinguished by their low permeability constitute the clay complex. Because of this reduced permeability, this complex is considered to have very low permeability; the average thickness is in the tens of metres. This complex outcrops within the central and southern sectors of the study area (Fig. 4) where it is covered by a coarse-grained complex, which is described below.

The sand-conglomerate-calcarenite complex includes terraced marine deposits and alluvial-coastal successions, and it has low to high permeability because of variations in porosity. The complex thickness is generally less than 30 m, and it is an outcropping complex that drapes other complexes. This complex widely lies on the clay complex and constitutes the shallow aquifers, which are narrow and/or discontinuous and have a shallow and medium permeability on average because of the material porosity. Therefore, these aquifers can be considered of secondary hydrogeological relevance.

A wide and deep limestone aquifer (main aquifer) occurs in the studied area (Fig. 5). Piezometric data from the 70s, a period in which the level of groundwater exploitation was low, were validated (WMO 1994; Uil et al. 1999). These data can be considered representative of the natural flow conditions (negligible anthropic effect), and data from 427 wells in the limestone aquifer were used to assess the piezometric surface and assess the groundwater divide of the Mar Piccolo hydrogeological basin (Fig. 1). The groundwater base level of this aquifer corresponds to the sea level, and the piezometric heads drop rapidly from values above 10 m.a.s.l. in the inner areas to values close to 1 m.a.s.l. near the shoreline. Moreover, the spatial trend of the piezometric surfaces is deeply influenced by the draining effect of the coastal springs (subaerial and submarine springs); therefore, the main direction of the groundwater outflows are primarily towards the Mar Piccolo basin.

Because of the presence of the clay complex on the deep aquifer, the shallow aquifers can be disregarded in quantitative assessments related to direct contributions to the hydrological budget of the Mar Piccolo basin. Both aquifer types are naturally recharged by rainfall infiltration, and the contribution of drainage network exchanges or other aquifers appears to be almost negligible.

Survey activities and data discussion

Two types of surveys were performed: one to validate the geological and hydrogeological conceptualisation as previously described and another to assess the groundwater, seawater and subaerial springs by performing water sampling, in situ measurements of spring yield outflow of subaerial springs and chemical and physical water characteristics. The survey was conducted five times from March 2013 to October 2015.

Six main springs were recognised in the Mar Piccolo hydrogeological basin: subaerial springs (Galeso, Battentieri and Riso) and submarine springs (Citro Galeso, Citrello and Citro Le Copre) (Fig. 4).

The Galeso spring (n. 1 in Fig. 4) consists of a wide outflowing area that is topographically depressed and covered by marsh vegetation, and it produces a perennial stream that is approximately 900 m long and flows into the eastern bay of

the Mar Piccolo basin. The Battentieri and Riso spring areas (n. 2 and n. 3 in Fig. 4) are similar to that of the Galeso spring but narrower. The Battentieri spring is located 300 m from the shoreline and creates a narrow and almost natural pool that is used for recreational purposes. This natural pool includes a low waterfall located close to an ancient building, which was historically used as a convent, through which a portion of the spring water naturally flows.

Discontinuous historical data were available for the outflow of certain subaerial coastal springs (Servizio 1953). The outflow of the Citro Galeso spring has been measured several times (Cotecchia et al. 1989), and the yield of two spring outlets located close to the Citro Citrello spring (a schematic map with low accuracy is available in Stefanon and Cotecchia 1969) has only been determined once, with an outflow yield of 0.350 m^3/s. Unvalidated data from recent regional monitoring activity were disregarded (WMO 1994; Uil et al. 1999). Therefore, the historical monitoring data of the outflow yields were integrated through direct field measurements during the water sampling surveys. A single-point Doppler current meter which permits accurate 3D velocity measurements as function of water temperature and salinity (accuracy of 1 % of the measured velocity from 10^{-4} to 4.5 m/s) was used. The statistics of entire spring outflow dataset is summarised in Table 1, and the highest subaerial spring yield was observed for the Galeso spring (n. 1 in Fig. 4). The low value of standard deviation of spring outflow seems due to the wide extension, high thickness and, as a whole, high storage of the deep limestone aquifer.

Measurements of the water temperature, specific electrical conductivity (EC), dissolved oxygen (DO), pH and redox potential (Eh) were performed. An inland well that is representative of pure fresh groundwater (PFG) samples of the limestone aquifer was selected as a reference (Polemio et al. 2009). The seawater and pure fresh groundwater were sampled, and a comparison was performed with the geochemical composition of the spring water.

The ion concentrations were determined through ion chromatography methods with separate conductometric detection of cations and anions (Table 2). The total alkalinity was determined by titration with 0.1 N HCl to a pH of 4.5. For brevity, Table 2 only shows the hydro-geochemical results of the water sampled during the March 2014 survey (the ratio among ranges and ion concentrations is less than 30 % for each ion/location, and it accounts for seasonal variability). The distribution of the main ion concentrations in the sampled waters is shown in Fig. 6.

Table 1 Spring outflow yield statistics (m^3/s)

Spring	1 Galeso	2 Battentieri	3 Riso	4 Citro Galeso
Mean	0.5	0.2	0.1	0.7
Standard deviation	0.06	0.04	0.02	0.12
Start	1926	1926	1926	1988
End	2013	2013	2013	1989
Measures	85	58	45	5

The groundwater within carbonate aquifers is generally characterised by a predominance of calcium and bicarbonate ions because of the dissolution of calcite and dolomite. Dolomite has poor solubility compared with calcite. In a system containing calcite, dolomite dissolution may be congruent or incongruent depending on the concentration of calcium derived from calcite (Wigley 1973). If water is subsaturated with calcite, congruent dissolution of dolomite occurs.

Spring groundwater is subsaturated with calcite and dolomite (Table 2). These waters are characterised by high values of electrical conductivity and high concentrations of alkaline ions (Na^+ and K^+) and chloride ions and show typical chemical characteristics of fresh groundwater contaminated by seawater intrusion. These waters could be classified as Na-Cl-rich. The geochemical composition of the spring groundwater can be considered a mixture of seawater (sample S) and pure fresh groundwater sampled from the PFG well (sample W, Table 2 and Fig. 6). The fraction of seawater (f_{sea}) in each sample was calculated from the concentration of chloride ions (mmol/L), which is considered a conservative ion in the mixing process (Appelo and Postma. 2005):

$$f_{sea} = \frac{m_{Cl^-,sample} - m_{Cl^-,fresh}}{m_{Cl^-,sea} - m_{Cl^-,fresh}} \quad (1)$$

The subaerial spring groundwater of Mar Piccolo shows a mixing ratio with seawater between 5 % and 7.2 % (Table 2).

The expected concentration of the different ions ($m_{i.\ mix}$) resulting from the mixture between freshwater and saltwater can be calculated by:

$$m_{i,mix} = f_{sea} \cdot m_{i,sea} + (1 - f_{sea}) \cdot m_{i,fresh} \quad (2)$$

where $m_{i.sea}$ and $m_{i.fresh}$ are the seawater and freshwater concentrations of the ion i (mmol/L), respectively. The enrichment or depletion ($m_{i,react}$) of the ion i is then obtained by:

$$m_{i,react} = m_{i,sample} - m_{i,mix} \quad (3)$$

where $m_{i.react}$ may be a positive or negative value or equal to zero (only mixing). Positive or negative values of $m_{i,react}$ indicate the presence of geochemical processes that modify the water hydrochemistry in addition to simple mixing. Spring groundwater shows an enrichment of calcium and hydrogen bicarbonate together with depletion of magnesium ions (Table 2), and these effects could be related to the dolomitisation of the limestone induced by seawater intrusion, as suggested by Hanshaw et al. (1971).

Radiocarbon of the Galeso spring was determined by Accelerator Mass Spectrometry (AMS). The result was 40.3 +/- 0.2 pMC (percentage of modern carbon, ^{14}C). The value of $^{13}C/^{12}C$ ratio, obtained from the analysis and used for the

Table 2 In situ measurements and laboratory analysis results and calculations for the springs, pure fresh groundwater sampled at a reference well and seawater. Results of the first survey (March 2014); for the sampling location, refer to Fig. 4

Sample	Pure fresh groundwater	1 Galeso Spring	2 Battentieri Spring	3 Riso Spring	Mar Piccolo sea water
In situ measurements					
T (°C)	18.2	18.5	18.0	17.2	20.5
pH	7.75	6.98	7.05	7.02	7.33
EC (μS/cm at 25 °C)	510	3830	5300	3910	48300
Eh (mV)	225	197	176	153	52
DO (mg/L)	5.78	4.21	5.86	5.12	6.29
Ion concentrations (mg/L)					
Li^+	<0.05	0.03	0.04	0.02	0.15
Na^+	12.5	569.5	824.5	575.9	11160
K^+	3.19	17.64	30.13	22.03	337.10
Ca^{2+}	57.9	123.0	141.7	125.0	408.7
Mg^{2+}	24.2	75.0	98.0	77.8	1297.0
F^-	0.27	3.68	3.67	2.89	1.52
Cl^-	12.9	1060.5	1638.7	1068.7	21024.0
Br^-	0.05	4.22	5.99	4.20	69.40
NO_3^-	23.7	16.8	13.7	22.5	0.98
HCO_3^-	281	354	372	366	171
SO_4^{2-}	7.5	160.6	222.6	156.2	2458.0
Saturation index (SI) and seawater mixing fraction and reaction					
$SI_{calcite}$	0.40	−0.23	−0.14	−0.17	−0.07
$SI_{dolomite}$	0.85	−0.30	−0.06	−0.17	0.71
f_{sea} %	0	5.0	5.0	7.2	100
$Ca^{2+}{}_{mix}$	–	1.9	2.1	1.9	–
$Ca^{2+}{}_{react}$	–	1.2	1.4	1.2	–
$Mg^{2+}{}_{mix}$	–	3.6	4.8	3.7	–
$Mg^{2+}{}_{react}$	–	−0.6	−0.8	−0.5	–
$HCO_3^-{}_{mix}$	–	4.4	4.4	4.4	–
$HCO_3^-{}_{react}$	–	1.4	1.7	1.6	–

radiocarbon age corrections, was −9.6‰. The corrected groundwater age was assessed with the models of Pearson (1965) and Tamers (1975); it was equal to 1445 and 2055 years BP, respectively. A_0, the activity at the time zero, was assessed with modelling assumptions based on bibliographical sources of data, except for the alkalinity (5.8 mmol/L), measured on site. Modelling assumptions were as follows: concerning CO_2 of soil, the $\delta^{13}C$ and ^{14}C activities equal to −20‰ and 100 pMC, respectively; the $\delta^{13}C$ and ^{14}C activities of soil reacting mineral or solid phase equal to 0‰ and 0 pMC, respectively. Due the type of available data, the corrected age of Pearson should be considered more appropriate and reliable.

Model results and spring water budget

The hydrogeological conceptualisation was used to construct the 3D groundwater numerical model. The model includes an area of approximately 978 km^2 with four hydrogeological complexes, and it was defined using 9 layers, which produced approximately 400,000 cells, with squared horizontal faces of up to 150 m long and a variable cell thickness of up to 80 m. The simulated altitude ranged from 524 (inland) to −250 m.a.s.l. (Figs. 4 and 5).

Modelling was primarily conducted to define the flow domain under natural conditions and the entire groundwater contribution to the Mar Piccolo water balance. Thus, the program MODFLOW was selected and implemented with the complementary codes PEST and MODPATH.

The hydrogeological parameters (except the infiltration coefficient and hydraulic conductivity of the limestone aquifer) (Table 3) were defined for each hydrogeological complex using data from the literature (Civita 2005). Data from the literature on the infiltration coefficient were validated with detailed hydrogeological studies of similar hydrogeological basins (Civita 2005; Romanazzi and Polemio 2013). The

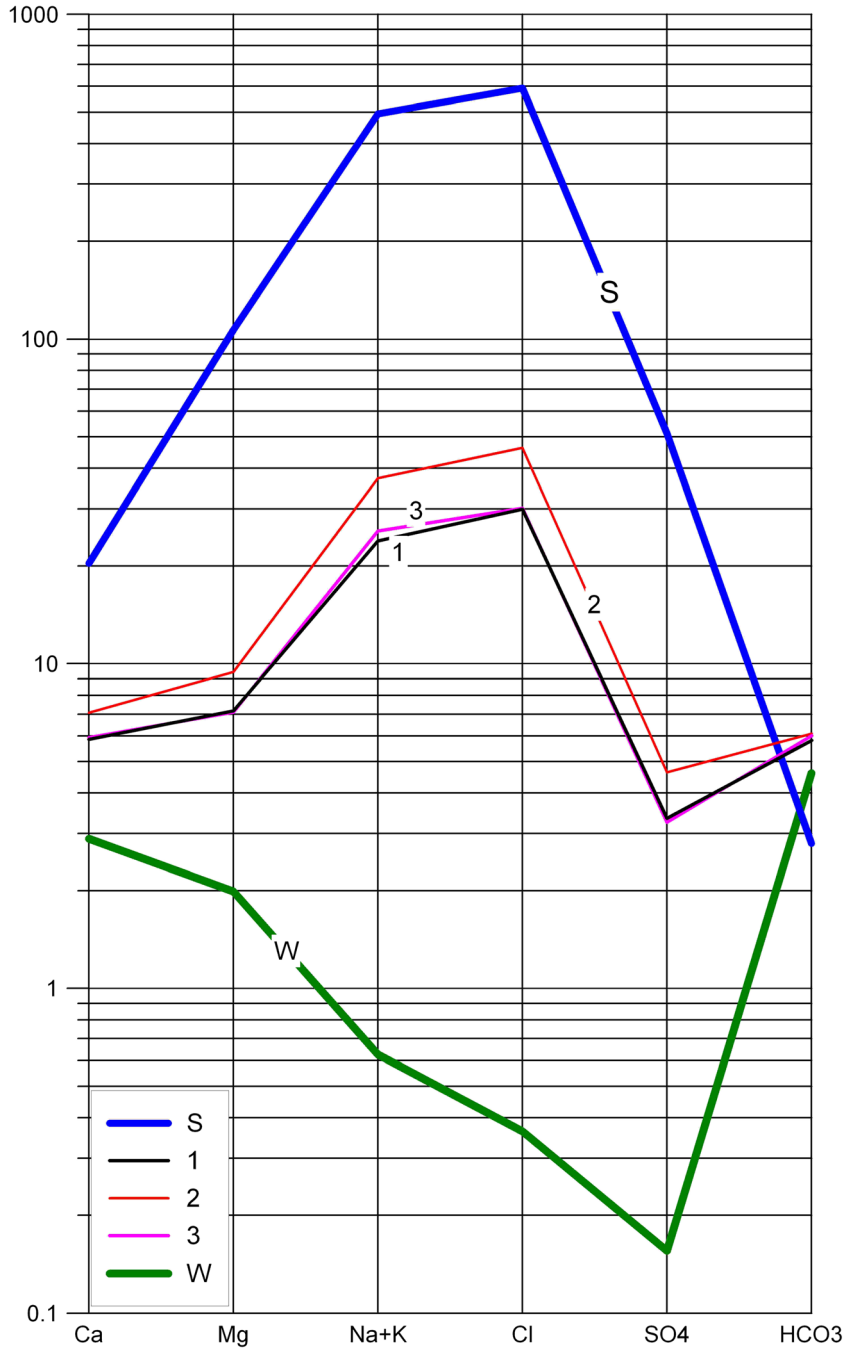

Fig. 6 Schoeller diagram. *1*) Galeso Spring, *2*) Battentieri Spring, *3*) Riso Spring, *W*) pure fresh groundwater (PFG) of the reference well of the limestone aquifer, and *S*) Mar Piccolo sea water; results of the October 2014 survey (Table 2)

Table 3 Hydrogeological complex parameters. Kx, Ky and Kz are the principal components of hydraulic conductivity (m/s), n_e is the effective porosity, Sy is the specific yield, Ss is the specific storage (1/m), and (C_i) is the infiltration coefficient. The values of hydraulic conductivity were defined after calibration

Complex	Kx=Ky=10Kz	n_e	Sy	Ss	C_i
Limestone	$5\ 10^{-5}$ to $1\ 10^{-2}$	0.05	0.14	$1*10^{-7}$	0.9
Calcarenite	$5*10^{-5}$	0.25	0.15	$6.3*10^{-5}$	0.5
Clay	$1*10^{-7}$	0.02	0.02	0.001	0.2
Sand, conglomerate and calcarenite	$1*10^{-5}$	0.2	0.2	$3.2*10^{-4}$	0.5

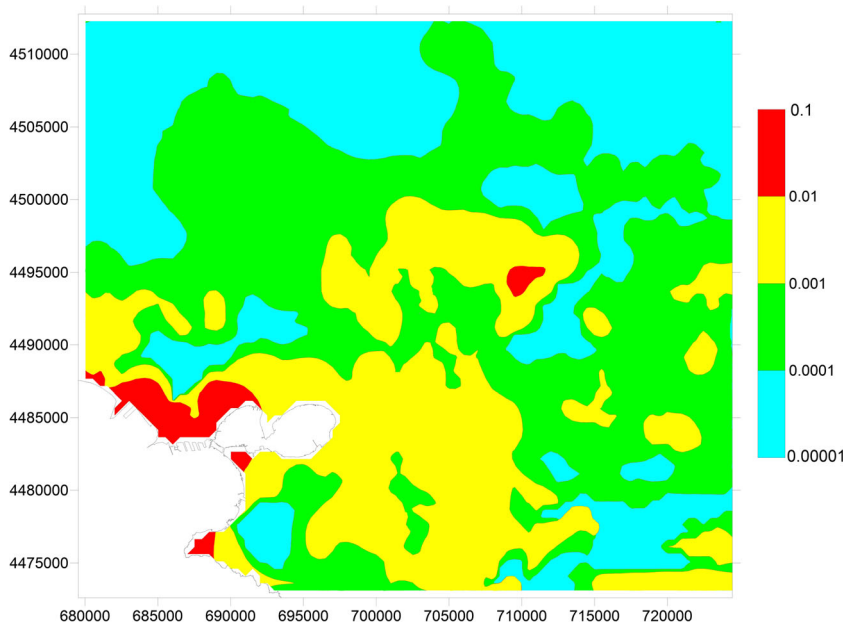

Fig. 7 Hydrogeological conductivity map of the limestone complex (m/s)

hydrogeological conductivity map was based on 886 point values derived from pumping tests and used as the model input (Fig. 7). As shown in the figure, the hydraulic conductivity tends to increase from inland areas to the coast and from NW to SE. Moreover, the hydraulic conductivity was optimised by the model calibration for each hydrogeological complex.

Six main springs (Fig. 4) were simulated with the model using a Cauchy condition, coastal/marine cells were modelled with a Dirichlet condition and inactive domains (cells outside the hydrogeological boundary) were modelled with no flow cells (Anderson and Woessner 1992); the remaining active cells did not have boundary conditions.

The limestone aquifer is naturally recharged by rainfall infiltration, which was assessed according to the mean hydrological budget of the hydrogeological basin. The mean monthly rainfall and temperature data for 7 temperature and rain gauges were considered. The selected data period was from 1930 to 1975 because this period was not particularly affected by climate change effects (Polemio and Casarano 2008). The measured annual rainfall (from 523 to 848 mm) and temperature (from 11 to 19 °C) in the hydrogeological basin were used to define a linear correlation with altitude (coefficient of determination (R^2) equal to 0.79 and 0.69, respectively). Using a cell by cell approach, which is described in detail by Romanazzi and Polemio (2013), the altitude and climate data were merged; the mean annual spatial value of net rainfall was 177 mm for the hydrogeological basin. The recharge was calculated by multiplying the infiltration coefficient by the net rainfall cell values, which were assessed due to the calculation of the actual evapotranspiration with the traditional Thornthwaite and Mather method. The mean annual recharge was 97.2 10^6 m^3 for the entire hydrogeological basin, equal to 99.4 mm or 14.5 % of rainfall (the mean monthly recharge was null from April to November and almost homogenously distributed from December to March).

Using piezometric surface data from the 1970s as the initial condition (Fig. 1), a steady-state model was calibrated. Hydraulic conductivity was calibrated with a trial and error approach in the Cauchy-condition cells and with the PEST code

Table 4 Calculated values of Q_i and mean outflow yield of spring *i*, where *i* is from 1 to 6, and Q_{im}, and mean monthly springs outflow per month (m^3/s)

Spring	Q_i	Jan	Feb	Mar	Apr	May	Jun	Jul	Aug	Sep	Oct	Nov	Dec
Galeso	0.447	0.447	0.450	0.453	0.450	0.448	0.448	0.447	0.446	0.445	0.444	0.443	0.443
Battentieri	0.198	0.196	0.199	0.202	0.201	0.202	0.199	0.200	0.198	0.196	0.195	0.194	0.194
Riso	0.115	0.112	0.118	0.124	0.121	0.119	0.117	0.117	0.115	0.112	0.110	0.109	0.107
Citro Galeso	0.669	0.670	0.671	0.673	0.670	0.669	0.669	0.669	0.668	0.668	0.668	0.667	0.667
Citrello	0.321	0.321	0.323	0.325	0.323	0.322	0.321	0.321	0.320	0.319	0.320	0.318	0.318
Le Copre	0.664	0.663	0.668	0.670	0.667	0.666	0.665	0.665	0.663	0.661	0.661	0.660	0.659
Total	2.414	2.409	2.429	2.447	2.432	2.426	2.419	2.419	2.41	2.401	2.398	2.391	2.388

for the remainder of the aquifer using 45 monitoring wells (Anderson and Woessner 1992; Doherty 2002). The results of the calibration are as follows: correlation coefficient=0.9, root mean square (RMS)=10.9 % and average absolute error=2.85 m.

The calculated mean annual value Q_i of the outflow yield of each spring i, where i is from 1 to 6, was assessed (Table 4). Using the output of the steady-state model as the initial condition and monthly recharge values, a long-term transient model was designed to assess Q_{im} the mean monthly spring i outflow yield, where month *m* is a value from 1 to 12 representing January to December (Table 4). The transient duration was extended to year Y so that the final solution satisfies both of the following conditions:

$$\left| Q_i - \frac{1}{12}\sum_{m=1}^{12} Q_{imY} \right| < 0.001 \; Q_i \quad \forall i = 1,..6 \tag{4}$$

$$\frac{1}{12}\left| \sum_{m=1}^{12} Q_{im(Y-1)} - \sum_{m=1}^{12} Q_{imY} \right| < 0.0001 \sum_{m=1}^{12} Q_{im(Y-1)} \quad \forall i = 1,..6 \tag{5}$$

The monthly values of the last year *Y* can be considered the mean monthly outflow yield (a transient duration of 200 years was sufficient, Table 4). A low variability of mean monthly outflow of each spring was assessed; it seems due to the low variability of the mean monthly recharge and to the wide extension of the deep limestone aquifer; in any case, this low variability is in good agreement with the low standard deviation of measured spring outflows (Table 1).

Using the transient model, the main path flow lines and travel time were assessed (Fig. 8). The maximum travel time in the hydrogeological basin was equal to approximately 1500 years, almost matching with the spring groundwater age; it can be considered a good confirmation of the model reliability because of the extreme complexity of the simulated phenomena.

The yearly outflow from the main springs into the Mar Piccolo basin was 75.2 10^6 m^3. The yearly outflow and inflow caused by coastal cells (into or from the Ionian sea, including the Mar Piccolo) was approximately 31.73 10^6 m^3 and 9.73 10^6 m^3, respectively. The outflow by coastal cells is due to diffuse seepage and small submarine springs (*citri*). The inflow by coastal cells confirms the role of the current seawater intrusion; the amount of this inflow is roughly consistent with the fraction of seawater assessed by spring water analyses (Table 2).

Conclusions

The Mar Piccolo basin can be considered the drainage basin for the springs that are located along the coast and at the sea bottom and discharge groundwater from the deep limestone aquifer.

A literature analysis was performed that included data on the springs and lithological logs of several boreholes drilled in the studied area, and field surveys, hydrogeological monitoring and geochemical analyses of the water samples were performed to define the recharge basin of the Mar Piccolo springs and their hydrogeological characteristics. All of the data were implemented in the numerical model designed for the studied area to simulate and predict the groundwater flow conditions and characteristics. The numerical model was optimised to assess the groundwater outflow yield of the primary subaerial and submarine coastal springs into the sea basin.

The mean annual volume exchanged by the hydrogeological basin was assessed equal to 106.93 10^6 m^3 (as inflow 97.2 and 9.73 10^6 m^3 due to recharge and seawater intrusion respectively, as outflow 75.2 and 31.73 10^6 m^3 due to outflow by the main springs and diffuse seepage together with small submarine springs, respectively).

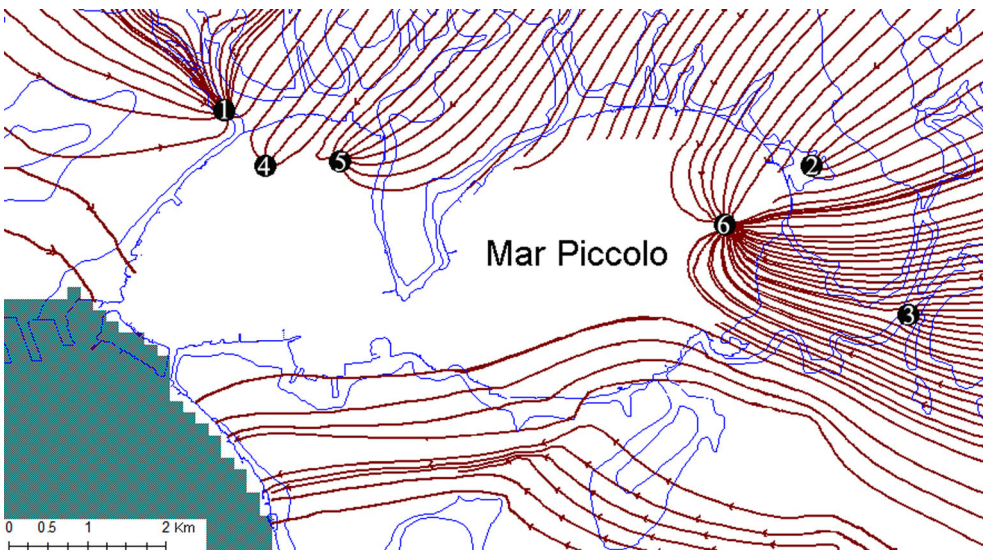

Fig. 8 Main path flow lines and travel times (displacement between two consecutive arrows corresponds to 10,000 days). Main springs: (*1*) Galeso, (*2*) Battentieri, (*3*) Riso, (*4*) Citro Galeso, (*5*) Citrello, (*6*) Citro Le Copre

The mean groundwater outflow yield was 2.41 m^3/s (75.2 10^6 m^3 per year); however, the total value of groundwater outflow into the Mar Piccolo may be underestimated because of the contribution of small *citri* or submarine springs and seepage by sea bottom. The absolute value of the residual between total amount of calculated and measured outflow of main springs (Tables 1 and 4) was 4.97 % of the total measured value; this result seems acceptable and almost justified by the accuracy level of available knowledge.

In addition, the geochemical data showed limited salinization of the groundwater outflowing from the subaerial coastal springs by seawater intrusion and a mixing ratio with seawater of less than 10 %. Apart from mixing, the groundwater composition of the subaerial springs of Mar Piccolo is controlled by the combined effects of calcite dissolution and ion exchange. Enrichment of calcium and hydrogen bicarbonate together with depletion of magnesium ions was observed. These effects seem due to the dolomitization of the limestone induced by seawater intrusion.

The highest travel time (approximately 1500 years) is so high to suggest the variability of the main chemical groundwater characteristics due to variability of natural conditions as climate change and/or sea level change will be very low over time. However, the results presented here will be improved with future research efforts.

Acknowledgments The activities described in this publication were funded by the Italian Flag Project "RITMARE - La Ricerca Italiana per il Mare" which was coordinated by the National Research Council and funded by the Ministry for Education, University and Research within the National Research Programme 2011–2013.

References

Abbo H, Shavit U, Markel D, Rimmer A (2003) A numerical study on the influence of fractured regions on lake/groundwater interaction; the lake Kinneret (Sea of Galilee) case. J Hydrol 283(1–4):225–243

Anderson MP, Woessner WW (1992) Applied Groundwater Modeling: Simulation of Flow and Advective Transport. Academic Press

Annichiarico C, Bottiglia F, Cardellicchio N, Di Leo A, Giandomenico S, Lopez L, Spada L (2009) Caratterizzazione chimico-fisica delle acque del Mar Piccolo di Taranto (campagna 2008). Rapporto Tecnico N.116/ISTTA/Chimica/CN/ aprile 2009. CNR-IAMC, Taranto

Appelo CAJ, Postma D (2005) Geochemistry, groundwater and pollution, 2nd edn. A.A. Balkema, Rotterdam

ASCE (1996) Hydrology handbook, manual and reports of engineering practice, 28. American Society of Civil Engineers, New York

Cardellicchio N, Buccolieri A, Giandomenico S, Lopez L, Pizzulli F, Spada L (2007) Organic pollutants (PAHs. PCBs) in sediments from the Mar Piccolo in Taranto (Ionian Sea. Southern Italy). Mar Pollut Bull 55:451–458

Castany G (1982) Principes et méthodes de l'hydrogéologie. Dunod, Paris

Cerruti A (1938) Le sorgenti sottomarine (Citri) del Mar Grande e Mar Piccolo di Taranto. Annali Istituto Superiore Navale Di Napoli, Napoli, p 7

Ciaranfi N, Pieri P, Ricchetti G (1988) Note alla carta geologica delle Murge e del Salento (Puglia centromeridionale). Mem Soc Geol Ital 41:449–460

Civita M (2005) Idrogeologia applicata ed ambientale. Casa Editrice Ambrosiana, Milan

CNR (1987) Neotectonic Map of ltaly, 114th edn. Quaderni della ricerca scientifica, Firenze, p 4

COST (2005) Cost Action 621 Groundwater management of coastal karst aquifers. European Commission, Directorate-General for Research. Report EUR 21366

Cotecchia V, Lollino G, Pagliarulo R, Stefanon A, Tadolini T, Trizzino R (1989) Studi e controlli in situ per la captazione della sorgente sottomarina Galeso. Mar Piccolo di Taranto. Conv Int Geoing Suolosottosuolo Torino 27–30:475–484

Cotecchia V, Grassi D, Polemio M (2005) Carbonate aquifers in Apulia and seawater intrusion. Giorn Geol 1:219–231

Doherty J (2002) PEST Model-independent parameter estimation. Watermark Numerical Computing

Fetter CW (2001) Applied hydrogeology, 4th edn. Prentice Hall, New Jersey

Hanshaw BB, Back W, Deike RG (1971) A geochemical hypothesis for dolomitization by groundwater. Econ Geol 66:710–724

Langevin CD (2003) Simulation of submarine ground water discharge to a marine estuary: Biscayne Bay: Florida. Ground Water 41(6):758–771

McDonald MG, Harbaugh AW (1988) A modular three-dimensional finite-difference ground-water flow model. Techniques of Water-Resources Investigations of the United States Geological Survey. 6

Panetta P, Dell'Angelo B (1975) I citri del Mar Piccolo di Taranto. Conchiglie 11(3–4):65–86

Pearson F.J (1965) Use of C-13/C-12 ratios to correct radiocarbon ages of material initially diluted by limestone. Proceedings of the 6th International Conference on Radiocarbon and Tritium Dating: 357 366

Polemio M (1998) Le calamità idrogeologiche dell'inverno 1995–96 nel territorio tarantino. In: Luino F (ed) International Conference "Prevention of hydrogeological Hazards: the role of scientific research", vol 2, Alba. CNR IRPI., pp 63–73

Polemio M, Casarano D (2008) Climate change, drought and groundwater availability in southern Italy. Geochem Soc Spec Publ 288:39–51

Polemio M, Limoni PP (2001) L'evoluzione dell'inquinamento salino delle acque sotterranee della Murgia e del Salento: Memorie della Società Geologica Italiana 56: 327–331

Polemio M, Limoni PP (2006) Groundwater pollution and risks for the coastal environment (southeastern Italy). In Predictions in Ungauged Basins: Promise and Progress (ed) Sivapalan M, Wagener T, Uhlenbrook S, Zehe E, Lakshmi V, Liang X, Tachikawa Y, and Kumar P. IAHS Publications 303: 477–486

Polemio M, Romanazzi L (1999) Numerical simulation of ground water protection works for industrial waste dump. Bull Eng Geol Environ 57:253–261. doi:10.1007/s100640050042

Polemio M, Dragone V, Limoni PP (2008) Salt contamination of Apulian aquifers: spatial and time trend. 19th SWIM & 3rd SWICA jointed meeting: Cagliari. 115–121

Polemio M, Dragone V, Limoni PP (2009) Monitoring and methods to analyse the groundwater quality degradation risk in coastal karstic aquifers (Apulia. Southern Italy). Environ Earth Sci (formerly Environ Geol) 58:299–312. doi:10.1007/s00254-008-1582-8

Pollock DW (1989) Documentation of computer programs to compute and display pathlines using results from the U.S. Geological Survey modular three-dimensional finite-difference ground-water flow model. Open File Report. 89–381

Romanazzi A, Polemio M (2013) Modelling of coastal karst aquifers for management support: a case study of Salento (Apulia. Italy). Ital J Eng Geol Environ 1:65–83

Sanford W, Langevin C, Polemio M, Povinec P (2007) Preface. In: A new focus on groundwater-seawater interactions. IAHS Publications (ed)Sanford W, Langevin C, Polemio M, Povinec P. IAHS Press 312: V-VI

Scanlon BR, Mace RE, Barrett ME, Smith B (2003) Can we simulate regional groundwater flow in a karst system using equivalent porous media models? Case study. Barton springs Edwards aquifer. USA. J Hydrol 276(1–4):137–158

Servizio Idrografico (1953) Le Sorgenti Italiane (Italian Springs. in Italian). Elenco e descrizione. Regione Pugliese. Pubbl. n.14 del Servizio Idrografico. l. Roma

Stefanon A, Cotecchia F (1969) Prime notizie sulle caratteristiche di efflusso e sulle modalità di investigazione delle sorgenti subacquee ai fini·di una loro captazione. Ric Sci 58:165–195

Tamers MA (1975) Validity of radiocarbon dates on ground water. Geophys Surv 2:217–239

Todd DK, Mays LW (2005) Groundwater hydrology. Wiley, New York

Uil H, Van Geer FC, Gehrels JC, Kloosterman FH (1999) State of the art on monitoring and assessment of groundwaters. UN/ECE Task Force on Monitoring & Assessment. Working Programme 1996/1999. Vol. 4. ISBN 9036952778 Delft, The Netherlands

UNESCO (2004) Submarine groundwater discharge. IHP Groundwater series n. 5

Wigley TML (1973) The incongruent dissolution of dolomite. Geochim Cosmochim Acta 37:1397–1402

WMO (1994) Guide to hydrological practices. Fifth edition. WMO No.168